ORGANOMETALLICS

Article

pubs.acs.org/Organometallics

Impact of Backbone Substituents on POCOP-Ni Pincer Complexes: A Structural, Spectroscopic, and Electrochemical Study

Boris Vabre, Denis M. Spasyuk, and Davit Zargarian*

Département de Chimie, Université de Montréal, Montréal (Québec), Canada H3C 3J7

Supporting Information

ABSTRACT: When treated at room temperature and in the presence of NEt_3 with $\{(i\text{-PrCN})NiBr_2\}_n$, the pincer-type ligands R-POC^{H}OP$^{R'}$ undergo direct C−H nickellation to give the pincer complexes (R-POCOP$^{R'}$)NiBr in 45−92% yields (R-POCOP = $\kappa^P,\kappa^C,\kappa^P$-$\{R_n$-2,6-$(R'_2PO)_2C_6H_{3-n}\}$; R_n = 4-OMe, 4-Me, 4-CO_2Me, 3-OMe, 3-CO_2Me, 3,5-t-Bu_2; R' = i-Pr, t-Bu). These complexes have been characterized by multinuclear NMR and UV−vis spectroscopy as well as single-crystal X-ray diffraction studies to delineate the impact of R and R' on Ni−ligand interactions. The solid-state structural data have revealed slightly shorter Ni−Br bonds in the complexes bearing a 4-CO_2Me substituent, shorter Ni−P bonds in the complex bearing t-Bu substituents at the 3- and 5-positions, and longer Ni−P bonds in complexes featuring OP(t-Bu)$_2$ donor moieties. The UV−vis spectra indicate that a 4-CO_2Me substituent causes a red-shift in the frequency of the MLCT bands (330−365 nm), whereas the ligand field transitions appearing in the 380−420 nm region are influenced primarily by the P-substituents. Cyclic voltammetry measurements have shown that the oxidation potentials of the title complexes are affected by P- and ring-substituents, oxidation being somewhat easier with t-Bu_2PO (vs i-Pr_2PO), OMe and Me (vs CO_2Me), and t-Bu (vs Cl). Moreover, oxidation potentials are affected more by the aromatic substituents at the 4-position vs those at the 3- and 5-positions.

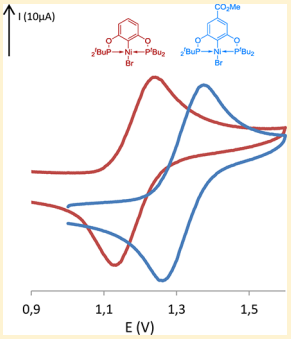

INTRODUCTION

Pincer complexes of nickel based on the 1,3-bis-(phosphinomethyl)- and 1,3-bis(aminomethyl)phenyl ligands were among the first pincer complexes reported by the groups of Shaw[1] and van Koten,[2] respectively. The organonickel chemistry of these so-called PCP- and NCN-type pincer ligands has received increasing scrutiny over the past three decades and led to the development of interesting applications based on both divalent and trivalent systems.[3] The past decade has also witnessed exciting discoveries emerging from the chemistry of nickel pincer complexes based on related new ligands such as $PC_{sp3}P$,[4] POCOP[5] and $POC_{sp3}OP$,[5b,c] POCN,[6] PNP,[7] and NNN[8] (Chart 1). These developments have underlined the possibility of fine-tuning the reactivities of nickel pincer complexes through modifications in donor moieties and the ligand backbone.

In this context, the groups of Guan, Goldberg, Peruzzini, and Hazeri have reported on the reactivities of (POCOP)Ni(H)[9] and (PCP)Ni(H)[10] as a function of P-substituents, while our group has reported on the structures and reactivities of charge-neutral and cationic PCP- and POCOP-type complexes of nickel as a function of different P-substituents and pincer backbones (aromatic vs aliphatic).[11] The impact of ring-substituents on the structures and reactivities of aromatic PCP- and POCOP-Ni complexes has not been examined in a systematic manner, but this issue is beginning to attract interest. For instance, Morales−Morales' group has reported very recently the synthesis of POCOP-type systems based on 4-n-dodecylresorcinol[12] and 1,3-dihydroxynaphthalene[13] and examined the effectiveness of the latter complex in Suzuki coupling, whereas Huang's group has studied the homocoupling of benzyl halides by (R-POCOP$^{R'}$)NiX (X = Cl, Br, I) to ascertain the influence of ring- and P-substituents R and R' on this reaction.[14] Our group has also shown that in the cationic complexes $[(POCOP)Ni(NCMe)]^+$ the P-substituents have greater influence on structures and reactivities relative to chloride substituents at the 3- and 5-positions (with respect to the metallated carbon).[11a] In contrast to these sporadic and limited studies for POCOP-Ni systems, the impact of ring- and P-substituents on the properties of POCOP-Ir complexes has

Chart 1.

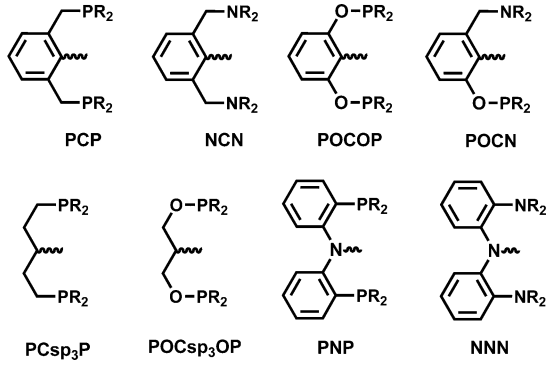

Received: October 9, 2012
Published: December 10, 2012

   dx.doi.org/10.1021/om3009475 | *Organometallics* 2012, 31, 8561−8570

Chart 2.

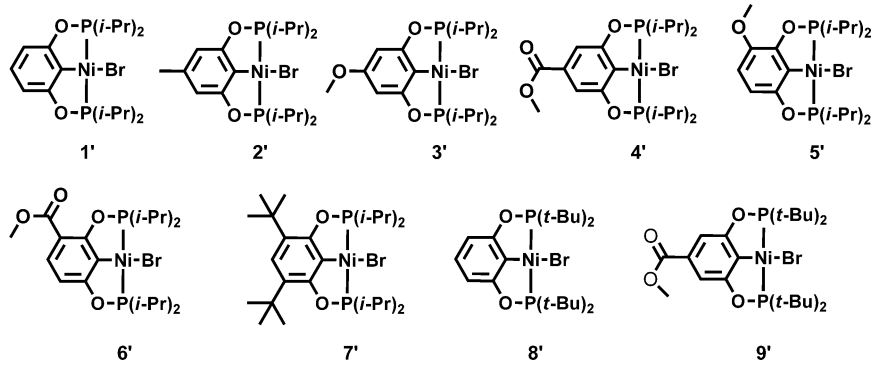

been investigated in much more detail.[15] Similar studies have been reported on NCN-Ni and NCN-Pt complexes.[16]

As a continuation of our investigations on the chemistry of POCOP-Ni complexes, we have set out to examine how the Ni center is influecned by ring-substituents, in particular those at the more sensitive 4-position (*para* with respect to the metalated carbon). The present report describes the synthesis and characterization of the complexes (R-POCOP$^{R'}$)NiBr where R and R′ represent, respectively, the substituents on the resorcinol ring and the phosphinite moiety (Chart 2). The impact of R and R′ on solid-state structures, electronic transitions, and electrochemical properties of these compounds will be discussed.

RESULTS AND DISCUSSION

The synthesis of *m*-phenylene-based POC^{H}OP ligands used in this study involved treating the doubly deprotonated resorcinol or its substituted derivatives R$_n$-POC^{H}OP with ClPR′$_2$ (Scheme 1)[17] and vacuum distillation of the oily products where possible; this methodology furnished six new ligands in 60−94% yields (Table 1). The new ligands were characterized by combustion analysis and NMR spectroscopy; the previously reported ligand POC^{H}OP$^{t\text{-Bu}}$ was also subjected to single-crystal X-ray diffraction analysis (vide infra). All the ligands were then treated with a small excess of $\{(i\text{-PrCN})NiBr_2\}_n$ in the presence of NEt_3 at ambient temperature to give the corresponding pincer complexes via a direct nickellation step (Scheme 1).[18] This straightforward methodology has allowed the preparation of eight new complexes in 45−92% yields (Table 1). It is interesting to note that the lowest yield is obtained from the ligand bearing bulky *t*-Bu substituents at the 3- and 5-positions on the ring (45% for complex **7′**), whereas in the case of *t*-Bu$_2$P-based derivatives placing a COOMe substituent at the *para* position appears to favor the yield (52% for complex **8′** vs 72% for complex **9′**).[19] The new complexes have been characterized by combustion analysis, NMR and UV−vis spectroscopy, and single -crystal diffraction studies (vide infra).

Scheme 1.

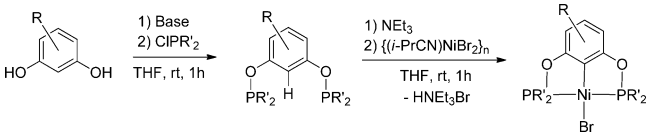

NMR Analyses. Assignments of NMR spectra for the new ligands and complexes were facilitated by comparison to the corresponding data obtained previously for fully characterized analogues.[5] Interestingly, the NMR data are only slightly affected by the ring-substituents R, as reflected in the fairly narrow ranges of ^{31}P δ values observed for all ligands (ca. 147−156 ppm) and complexes (ca. 188−192 ppm). In this regard, ^{31}P δ values of the ligand signals are more strongly affected as a result of nickellation, which causes a deshielding by ca. 40 ppm on average; the nearly linear relationship between ligand/complex ^{31}P chemical shift values is apparent from a plot of ^{31}P δ values provided as Supporting Information. In contrast, the impact of nickellation on the ^{13}C{^{1}H} δ values appears to be more complex: the aromatic carbon nucleus directly bonded to the Ni center experiences a downfield shift of ca. 17−24 ppm, whereas upfield shifts were noted for the remaining aromatic

Table 1. POCOP Ligands and Complexes Synthesized

		ligands			complexes		
R′	R	no.	yield (%)	^{31}P $\delta^{\dagger}$	no.	yield (%)	^{31}P δ^{b}
i-Pr		**1**[a]		149.0	**1′**[a]		188.2
	4-Me	**2**	85	148.9	**2′**	76	189.1
	4-OMe	**3**	70	147.5	**3′**	74	190.6
	4-CO$_2$Me	**4**	89	151.9	**4′**	92	190.6
	3-OMe	**5**	60	151.7, 157.2	**5′**	90	187.5 (d), 192.2 (d)[c]
	3-CO$_2$Me	**6**	94	151.2, 151.6	**6′**	86	190.4 (d), 192.1 (d)[d]
	3,5-*t*-Bu$_2$	**7**[a]		139.5	**7′**	45	185.2
t-Bu	H	**8**[a]		153.1	**8′**	57	191.0
	4-CO$_2$Me	**9**	63	155.8	**9′**	72	191.8

[a]Previously reported ligands/complexes. [b]Unless otherwise indicated, all signals are singlet resonances. [c]AB signal, $J_{PP} \approx 318$ Hz. [d]AB signal, $J_{PP} \approx 323$ Hz.

dx.doi.org/10.1021/om3009475 | *Organometallics* 2012, 31, 8561−8570

carbon nuclei (ca. 1−6 ppm) as well as most aromatic protons (ca. 0.2−0.4 ppm).

The ^{31}P NMR spectra of the nonsymmetrical ligands **5** and **6** and their complexes **5′** and **6′** were particularly instructive. The two inequivalent phosphinite moieties of these ligands showed two singlets appearing at fairly different chemical shifts in **5** (151.7 and 157.2 ppm), but very close to each other in **6** (151.1 and 151.6 ppm). The spectrum for complex **5′** displayed a "normal" AB pattern consisting of two doublets at 187.5 and 192.2 ppm ($^2J_{P-P}$ = 318 Hz; $\Delta\nu/J_{P-P} \approx 2.5$), whereas the spectrum for **6′** appeared to consist of two closely spaced singlets (192.06 and 192.13 ppm) instead of the expected AB doublets. The $^{31}P\{^1H\}$ NMR spectrum of a more concentrated sample recorded on a higher field instrument (ca. 202.5 MHz) showed a four-peak AB-type signal displaying very weak outer peaks (~1:20:20:1, Figure 1), which is presumably caused by

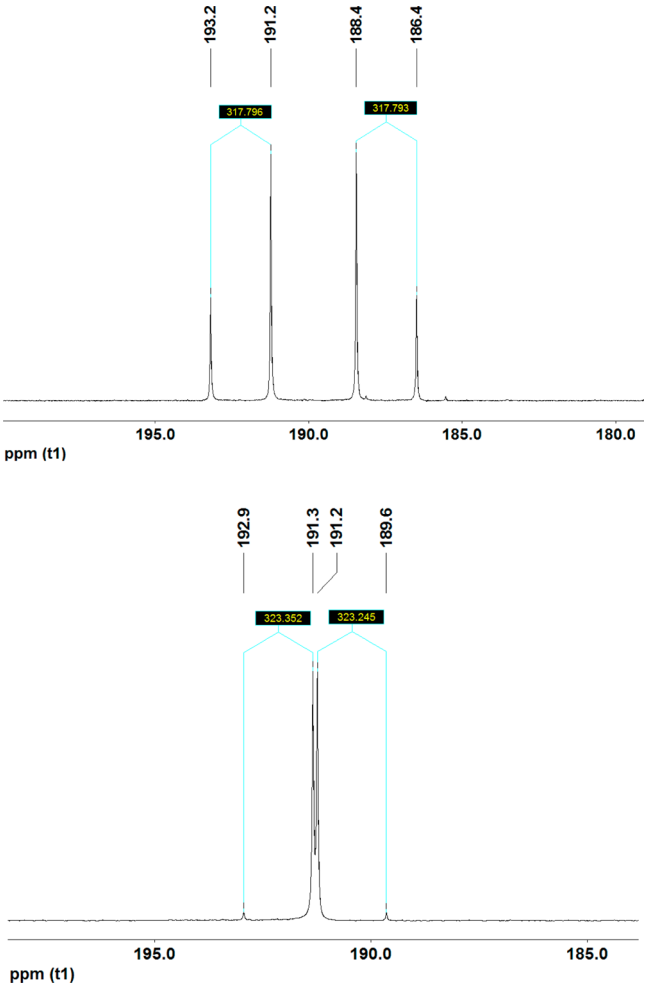

Figure 1. $^{31}P\{^1H\}$ NMR spectra of complexes **5′** (above) and **6′** (below).

the very similar chemical shifts of the two P nuclei and their large coupling constant ($\Delta\nu/J_{P-P} \approx 0.96$).[20] A similar "roof effect" has already been observed in an asymmetric PCP platinum pincer complex.[21]

Crystallographic Analyses. X-ray diffraction studies have been conducted on single crystals of complexes **3′**−**7′** as well as ligand **8**. Reliable structural data could not be obtained for compounds **5′** and **6′** due to the inferior quality of the single crystals obtained for these complexes, but the overall quality of the data was very good for all other products including complex **8′**, which displayed disordered *t*-Bu substituents.[22] The ORTEP diagrams are shown in Figure 2 (**8**) and Figure 3 (**3′**, **4′**, **7′**, and

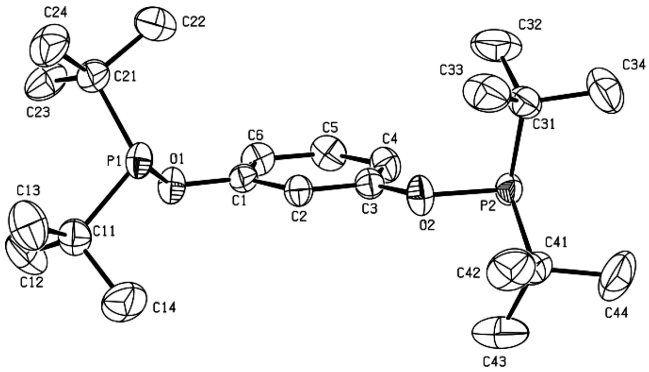

Figure 2. ORTEP diagram for ligand **8**. Thermal ellipsoids are shown at the 50% probability level. Hydrogen atoms are omitted for clarity.

8′), and the main structural parameters are listed in Table 2; details of the diffraction studies are listed in Table 1S and Table 2S (Supporting Information).

The *t*-Bu_2PO moieties in ligand **8** adopt positions that minimize steric interactions, with one moiety being in the plane of the aromatic ring, while the other phosphorus is out of plane by 0.798 Å. Comparison of the P−O distances in **8** and **8′** reveals a significant shrinkage (by 0.024 Å) upon complexation to nickel; this might arise from the P→Ni donation in the complexes that would enhance the dipolar character of the P−O bond. This is the first solid-state structure of a POCOP-type ligand.

The nickel center in all complexes adopts a distorted square-planar geometry due, primarily, to the small bite angle of the POCOP ligands (P−Ni−P ~164−165°). The Ni−C distances are fairly similar in all cases (~1.87−1.89 Å) as are Ni−Br distances (~2.31−2.34 Å), but the latter appear to be shortest in complexes bearing a 4-CO_2Me substituent. This point is best illustrated by comparing the Ni−Br distances in unsubstituted complexes **1′** (2.323(1) Å) and **8′** (2.338(2) Å) vs their 4-CO_2Me counterparts **4′** (2.312(1) Å) and **9′** (2.321(1) Å). The shorter Ni−Br distances in the complexes bearing electron-withdrawing substituents can be attributed to the weaker *trans* influence of the electron-depleted aryl rings.[23]

The Ni−P distances were found to be fairly insensitive to the ring-substituents R, but important variations were noted as a function of *P*-substituents R′ (~2.19 Å with *t*-Bu and ~2.14−2.16 with *i*-Pr). It is interesting to note that the shortest Ni−P bond distances in the *i*-Pr_2PO series are found in **7′**, implying that the presence of bulky *t*-Bu substituents on the 3- and 5-positions of the aromatic ring reinforces the Ni−P interactions.

Absorption Spectroscopy. UV−vis spectra were recorded for ca. 10^{-4} M CH_2Cl_2 solutions of the ligands (pale yellow) and complexes (yellow). The ligand spectra displayed multiple intense bands in the UV region below 250 nm, in addition to one or two bands of moderate intensity centered at higher wavelengths. The energies of the latter bands appear to be much more sensitive to the ring-substituents R than the *P*-substituents R′. For instance, the ligands bearing electron-releasing substituents or none absorb at 272−276 nm regardless of R′ (e.g., ligands **3**, **2**, and **8**), whereas those bearing the electron-withdrawing substituent 4-CO_2Me absorb at 306 nm (ligand **4**) or 308 nm (ligand **9**). We conclude that

dx.doi.org/10.1021/om3009475 | *Organometallics* 2012, 31, 8561−8570

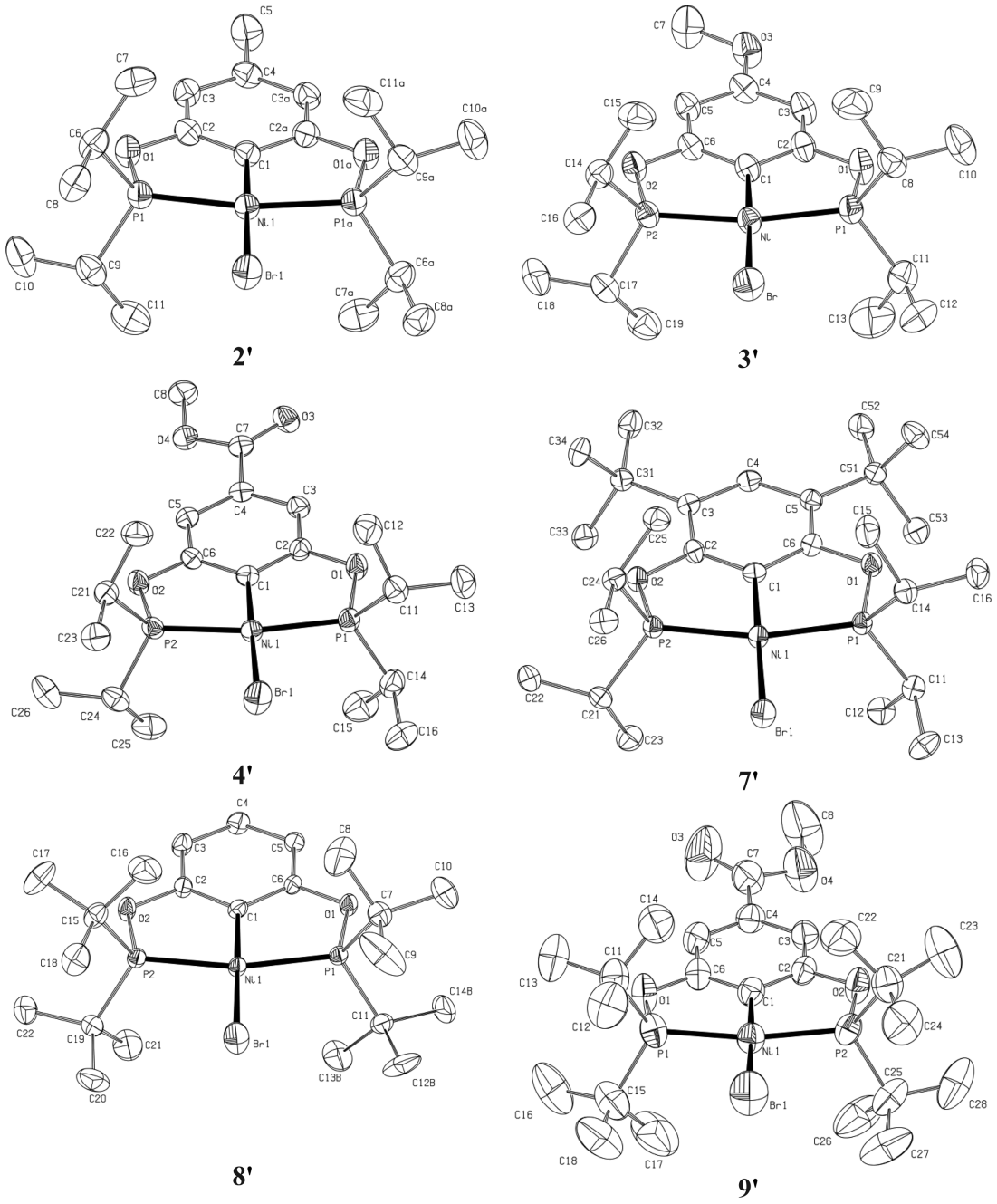

Figure 3. ORTEP diagrams for complexes **2′**–**4′** and **7′**–**9′**. Thermal ellipsoids are shown at the 50% probability level. Hydrogen atoms are omitted for clarity.

Table 2. Selected Bond Distances (Å) and Angles (deg) for Ligand 7 and Complexes 1′–4′, 7′, 8′, and 9′ (molecule 1)

compound	Ni–C	Ni–Br	Ni–P_1	Ni–P_2	P_1–Ni–P_2	P_1–O_1
1′[a]	1.885 (3)	2.323 (1)	2.153 (1)	2.142 (1)	164.92 (4)	1.663 (2)
2′	1.885 (3)	2.330 (1)	2.158 (1)		164.21 (3)	1.655 (2)
3′	1.877 (2)	2.319 (1)	2.155 (1)	2.152 (1)	164.65 (2)	1.663 (2)
4′	1.872 (2)	2.312 (1)	2.157 (1)	2.159 (1)	165.26 (2)	1.656 (2)
7′	1.892 (4)	2.320 (1)	2.139 (1)	2.143 (1)	165.06 (5)	1.650 (3)
8′	1.887 (2)	2.338 (2)	2.193 (1)	2.189 (1)	164.13 (3)	1.654 (2)
8						1.678 (1)
9′	1.877 (2)	2.321 (1)	2.189 (1)	2.194 (1)	164.58 (3)	1.652 (2)

[a]The data for **1′** are taken from ref 5b.

dx.doi.org/10.1021/om3009475 | *Organometallics* 2012, 31, 8561–8570

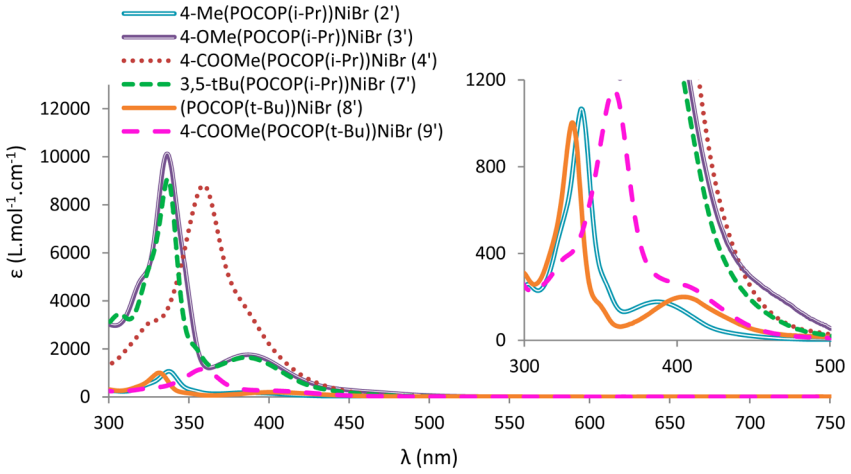

Figure 4. UV−vis spectra (CH_2Cl_2, rt) for complexes **2′**−**4′** and **7′**−**9′**.

these bands involve $\pi\rightarrow\pi^*$ transitions, and the difference between the frequencies observed for ligands **4** and **9**, on one hand, and all other ligands (ca. 4000 cm^{-1}) can be rationalized by considering that such transitions should be lower in energy when the buildup of charge in the excited state can be stabilized more effectively. In other words, ligands bearing the most effective electron-accepting ring-substituent should exhibit lower energy $\pi\rightarrow\pi^*$ transitions; a similar phenomenon is at work for the MLCT transitions in the complexes (vide infra).

Similarly to the ligands, the complexes displayed multiple high-intensity bands in the UV region, in addition to a few less intense bands in the regions 330−365 nm and 380−420 nm (Figure 4 and Table 3). Since the latter bands are absent in the ligand spectra, they can be assigned to electronic transitions of the complexes. Moreover, since the lowest energy bands are fairly insensitive to ring-substituents R and more sensitive to *P*-substituents R′, they can be attributed to spin-forbidden d−d transitions involving the ligand fields. This is anticipated for metal-centered transitions and most evident when we compare the energies of these bands for complexes **4′** and **9′** (ca. 26 000 vs 24 000 cm^{-1}). On the other hand, the more intense transitions in the region 330−365 that show greater sensitivity to the ring-substituents R are considered to be spin-allowed charge transfer bands (MLCT).[24]

Table 3. Absorption Spectral Data for Complexes 1′−9′

R′	R	no.	λ_{max} (nm) (ε, M^{-1} cm^{-1})	
i-Pr	H	**1′**	337(9409)	389(1975)
	4-Me	**2′**	338(1063)	396(164)
	4-OMe	**3′**	336(10109)	387(1753)
	4-CO_2Me	**4′**	362(8552)	384(3863)
	3-OMe	**5′**	337(900)	389(158)
	3-CO_2Me	**6′**	341(817)	397(157)
	3,5-*t*-Bu_2	**7′**	337(9060)	388(1631)
t-Bu		**8′**	334(916)	407(198)
	4-CO_2Me	**9′**	360(1043)	413(228)

The frequencies of MLCT transitions range from ca. 30 000 cm^{-1} in the spectra of complexes bearing either electron-releasing substituents (**2′**, **3′**, **5′**, and **7′**) or none (**1′** and **8′**) to ca. 28 000 cm^{-1} observed in the spectra of complexes **4′** and **9′**, bearing 4-CO_2Me substituents. Evidently, the largest electronic impact on MLCT transition frequencies (ca. 2000 cm^{-1}) is caused by 4-CO_2Me, and this observation can be rationalized as was discussed above for the $\pi\rightarrow\pi^*$ transitions of the unmetalated ligands. It is also worth noting that in some cases the energy of the MLCT band is more sensitive to the position of the ring-substituent R as opposed to its electronic character. Thus, the MLCT band of complex **6′** appears ca. 1600 cm^{-1} higher than that of **4′**, implying that the CO_2Me substituent exerts greater electronic influence at the 4- vs 3-position. As will be discussed below, the cyclic voltammetry measurements corroborate the greater impact of the 4-CO_2Me substituent on oxidation potentials of the complexes. The electron-releasing substituents Me, *t*-Bu, and OMe also influence the oxidation potentials of the complexes (vide infra), but they show little or no impact on the energies of the MLCT bands regardless of the substitution position. Thus, complexes **3′** and **5′**, bearing a OMe substituent at the 3- or 4-position, show MLCT bands at virtually identical energies.

Cyclic Voltammetry Measurements. Figure 5 shows the cyclic voltammograms of (R-POCOP$^{R'}$)NiBr, and Table 4 lists the potentials (vs ferrocene) in each case. Previous studies have established that PCP-,[4] POCOP-,[5b−d] and POCN-Ni[6a−c] complexes undergo one-electron oxidation of the nickel center that can be irreversible or reversible, depending on the specific complex and the conditions under which the measurements are made. The CV curves obtained for the complexes under discussion here show that the oxidation process is reversible for **2′** and **7**−**9′**, quasi-reversible for **3′** and **5′**, and irreversible for **6′**.

Comparison of the potentials for complexes **3′**−**7′** relative to complex **1′** (Table 4) provides valuable insights into the impact of ring- and *P*-substituents on one-electron oxidation in this family of complexes. Thus, the oxidation process is much easier for complexes containing electron-releasing substituents Me, OMe, and *t*-Bu (complexes **3′**, **2′**, **5′**, and **7′**). The greatest influence is exerted by the 4-OMe substituent, which lowers the oxidation potential by nearly 200 mV, whereas the 3-OMe has less influence.[25] By comparison, *P*-substituents appear to have less influence over the oxidation potential of these complexes, as seen from the nearly equal potentials of **1′** and **8′**. However, it is worth noting that the Ph_2PO analogue of these complexes shows a somewhat higher oxidation potential,[5d] as anticipated on account of the weaker donor aptitude of the Ph substituents. Finally, oxidation is more difficult for complexes containing electron-withdrawing ring-substituents (**4′**, **6′**, and **9′**), the

dx.doi.org/10.1021/om3009475 | *Organometallics* 2012, 31, 8561−8570

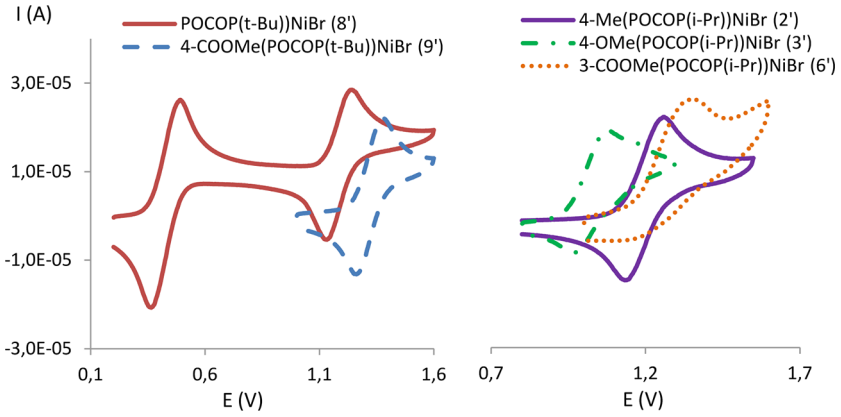

Figure 5. Cyclic voltammograms of **3′**, **2′**, **6′**, an equimolar mixture of **8′** and ferrocene, and **9′**. The measurements were carried out at 298 K on CH_2Cl_2 solutions containing the sample complexes (1 mM) and $[Bu_4N][PF_6]$ as electrolyte (0.1 M). A scan rate of 100 mV s^{-1} was used, and the potentials were referenced to the Cp_2Fe/Cp_2Fe^+ redox couple.

Table 4. Redox and Oxidation Potentials of (R-POCOP$^{R'}$)NiBr^a

R′	R	$E_{1/2}$ (mV)	E_{ox} (mV)
i-Pr	H (**1′**)		810
	4-Me (**2′**)	735	800
	4-OMe (**3′**)	565	620
	4-CO_2Me (**4′**)		940
	3-OMe (**5′**)	715	761
	3-CO_2Me (**6′**)		900
	3,5-*t*-Bu_2 (**7′**)	687	750
	3,5-Cl_2		840^b
t-Bu	H (**8′**)	750	800
	4-CO_2Me (**9′**)	860	920

^{a}See captions of Figure 2 or 3, or the Experimental section, for measurement details. ^{b}Reported in ref 11a.

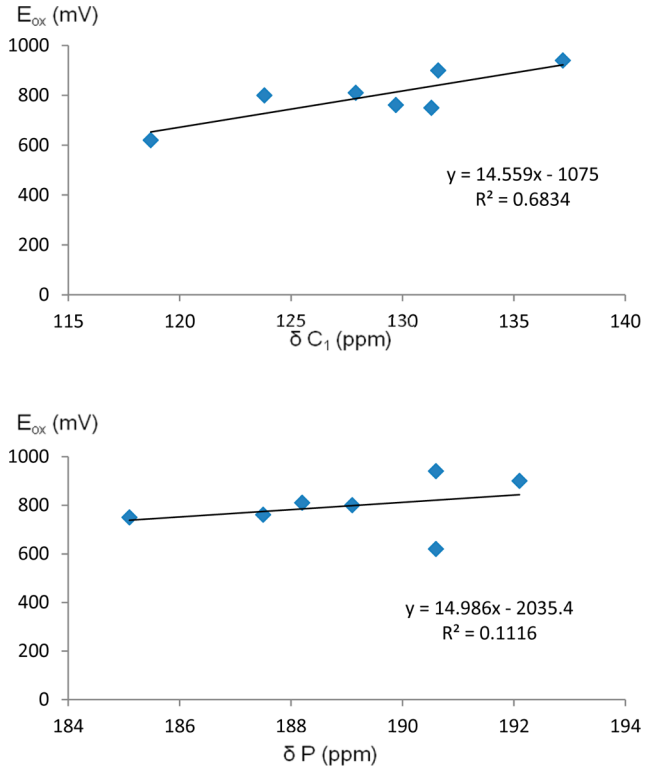

Figure 6. Plots of oxidation potentials vs NMR chemical shifts for the C_1 (above) and P (below) nuclei.

greatest influence (ca. 130 mV) being exerted by 4-CO_2Me. Thus, the electrochemical oxidation potential of (R-POCOP)-NiBr can be modulated over a range of 300 mV (**3′** vs **4′**) by judicious choice of the ring- substituents R.

The question arises as to how closely oxidation potentials reflect the level of electron density at the Ni center in the complexes under discussion. In the absence of reactivity data, it is tempting to seek other correlations that might shed light on this question. As discussed above, the energies of metal-centered electronic transitions are influenced by *P*-substituents, but they appear fairly insensitive to ring-substituents. We sought to establish whether or not there is any correlation between oxidation potentials obtained from CV measurements, on one hand, and the ^{13}C (δ C1) and ^{31}P chemical shifts on the other. Figure 6 shows plots of the ^{13}C and ^{31}P chemical shifts of various complexes against the corresponding oxidation potentials. These plots reveal a moderate degree of correlation between E_{ox} and δ C1 but a much more tenuous correlation with ^{31}P chemical shifts.

CONCLUSION

A previous study helped establish that substituents placed on the aromatic ring of resorcinol-based POCOP-type ligands can influence the nickellation step, leading to the formation of pincer complexes.[17] The present study is the first systematic attempt to measure the influence of ring-substituents on the electronics of the Ni center as manifested in its spectral, structural, and redox properties. Our findings point to a strong correlation between the redox potential of a given complex (R-POCOP)NiBr and the electronic nature of the ring-substituent R placed at the *para* position with respect to the nickellated carbon. An observable impact was also observed in the electronic spectra of the complexes bearing electron-withdrawing substituents COOMe at the 3- or 4-positions. On the other hand, the electronic properties of ring-substituents appear to have little or no impact on solid-state structures, but the steric bulk of the *t*-Bu substituents at the 3- and 5-positions appears to reinforce Ni−P interactions. The insights gleaned from the present study will help us design future investigations aimed at probing the impact of ring-substituents on the reactivities of this family of complexes.

dx.doi.org/10.1021/om3009475 | *Organometallics* 2012, 31, 8561−8570

EXPERIMENTAL SECTION

General Procedures. Unless otherwise indicated, all manipulations were carried out under a nitrogen atmosphere using standard Schlenk and glovebox techniques. Solvents were dried by passage over activated alumina contained in MBRAUN systems. Triethylamine was dried by distillation over CaH_2. The reagents isobutyronitrile, nickel powder, bromine, ClP(*i*-Pr)$_2$, ClP(*t*-Bu)$_2$, ClP(Ph)$_2$, 5-methyl-1,3-benzenediol, 4,6-dichloro-1,3-benzenediol, methyl 2,4-dihydroxybenzoate, methyl 3,5-dihydroxybenzoate, and NaH were purchased from Sigma-Aldrich and used without further purification. 5-Methoxyresorcinol was purchased from Chemsavers. 4-Methoxyresorcinol has been synthesized following a published procedure.[26]

Most NMR spectra were recorded at 400 (^{1}H) and 161.9 MHz (^{31}P) using a Bruker AV400rg spectrometer or at 400 (^{1}H) and 100.56 MHz (^{13}C{^{1}H}) using a Bruker ARX400 spectrometer. The ^{31}P{^{1}H} NMR spectrum of complex **6′** was recorded at 202.5 MHz using a Bruker AV500 spectrometer. Chemical shift values are reported in ppm (δ) and referenced internally to the residual solvent signals (^{1}H and ^{13}C: 7.26 and 77.16 ppm for $CDCl_3$; 7.16 and 128.06 ppm for C_6D_6) or externally (^{31}P, H_3PO_4 in D_2O, δ = 0). Coupling constants are reported in Hz. UV/vis spectra were measured on a Varian Cary 500i. The IR spectra were recorded on a Bruker Alpha-P FTIR (4000−400 cm^{-1}). The elemental analyses were performed by the Laboratoire d'Analyse Élémentaire, Département de Chimie, Université de Montréal.

{(*i*-PrCN)NiBr$_2$}$_n$. To a suspension of nickel powder (1 g, 17.04 mmol) in isobutyronitrile (50 mL) at 0 °C was added bromine dropwise (1.00 mL, 19.05 mmol), which caused a color change to green after a few minutes. Stirring the reaction mixture overnight at room temperature, followed by filtration, washing of the solid residue with Et_2O (2 × 25 mL), and drying under vacuum gave the desired product as a beige powder (4.58 g, 98%). This compound must be protected from ambient atmosphere, because it appears to be hygroscopic: the beige powder turns green after overnight exposure to air and becomes a green liquid after days. This compound has been identified based on its IR spectrum and elemental analysis. Multiple attempts to grow crystals of this compound have failed to produce single crystals. IR (cm^{-1}): 2974m, 2914m, 2864w, 2288vs, 1452vs, 1387w, 1367w, 1314w, 1278w, 1168w, 1103vs, 936w, 915w, 774w, 571w, 556s. Anal. Calcd for $C_4H_7Br_2NNi$ (287.61): N, 4.87 ; C, 16.70 ; H, 2.45. Found: N, 4.85; C, 17.00; H, 2.42. UV−vis (^{i}PrCN, 1.66 × 10^{-3} M) [λ_{max}, nm (ε, L mol^{-1} cm^{-1})]: 648 (103), 381(609), 313(1429), 284 (2001), 247 (1182), 223 (1885). $T_{decomposition}$ = 155 °C.

General Procedure for Synthesis of Ligands. We have followed previously published procedures for the synthesis of ligands **1**[15b] and **7**.[27] Ligand **9** was prepared using the same method as reported for **8**,[15c] whereas the remaining ligands were prepared using slightly modified versions of these procedures, as described below.

1,3-(*i*-Pr$_2$PO)$_2$-5-OMe-C$_6$H$_3$, 3. Dropwise addition of ClP(*i*-Pr)$_2$ (2.56 mL, 16.13 mmol) to a solution of 5-methoxyresorcinol (1.13 g, 8.06 mmol) and NEt_3 (2.47 mL, 17.7 mmol) in THF (50 mL) led to the formation of a white precipitate. The reaction mixture was stirred at room temperature for 1 h, followed by removal of the volatiles and extraction of the solid residues with hexane (3 × 25 mL) to give the crude product as a pale yellow oil (0.93 g, 70%). This material, which was shown by NMR spectroscopy to be greater than 98% pure, was used for the synthesis of the target complexes without further purification. ^{1}H NMR (400 MHz, C_6D_6): δ 0.97 (dd, J_{HP} = 19.6, J_{HH} = 7.2, 12H, CH(CH_3)$_2$), 1.13 (dd, J_{HP} = 10.4, J_{HH} = 7.0, 12H, CH(CH_3)$_2$), 1.74 (dh, J_{HP} = 2.5, J_{HH} = 7.0, 4H, PC*H*(CH$_3$)$_2$) 3.30 (s, 3H, OCH_3), 6.70 (m, 2H, *Ar*), 7.13 (m, 1H, *Ar*). ^{31}P{^{1}H} NMR (162 MHz, C_6D_6): δ 147.5 (s). ^{13}C{^{1}H} NMR (101 MHz, C_6D_6): δ 17.15 (d, J_{CP} = 8.6, 4C, CH_3), 17.9 (d, J_{CP} = 20.6, 4C, CH_3), 28.6 (d, J_{CP} = 18.5, 4C, PCH(CH$_3$)$_2$), 54.9 (s, 1C, OCH$_3$), 98.8 (d, J_{PC} = 11.0, 2C, 4,6-C$_{Ar}$), 101.9 (t, J_{PC} = 12.0, 1C, 2-C$_{Ar}$), 161.7 (d, J_{PC} = 9.4, 2C, C$_{Ar}$OP), 162.0 (s, 1C, C$_{Ar}$OMe). Anal. Calcd for $C_{19}H_{34}O_2P_2$ (372.42): C, 61.28 ; H, 9.20. Found: C, 60.73; H, 9.30.

1,3-(*i*-Pr$_2$PO)-5-Me-C$_6$H$_3$, 2. This ligand (a colorless oil) was prepared in 85% yield (2.45 g) using the same procedure described for the synthesis of **3**. ^{1}H NMR (300 MHz, $CDCl_3$): δ 1.09 (d, J_{HH} = 7.2, CH(CH_3)$_2$, 6H), 1.13 (d, J_{HH} = 7.2, CH(CH_3)$_2$, 6H), 1.17 (d, J_{HH} = 7.0, CH(CH_3)$_2$, 6H), 1.19 (d, J_{HH} = 7.0, CH(CH_3)$_2$, 6H), 1.92 (dh, J_{HP} = 2.2, J_{HH} = 7.1, 4H, PC*H*(CH$_3$)$_2$) 2.28 (s,CH_3, 3H), 6.58 (m, *Ar*, 2H), 6.72 (m, *Ar*, 1H). ^{31}P{^{1}H} NMR (162 MHz, $CDCl_3$): δ 148.9 (s). ^{13}C{^{1}H} NMR (101 MHz, $CDCl_3$): δ 17.10 (d, J_{CP} = 8.5, 4C, CH_3), 17.8 (d, J_{CP} = 20.2, 4C, CH_3), 21.6 (s, 1C, CH_3), 28.35 (d, J_{CP} = 17.5, 4C, PCH(CH$_3$)$_2$), 106.3 (t, J_{PC} = 10.36, 1C, 2-C$_{Ar}$), 112.7 (d, J_{PC} = 10.7, 2C, 4,6-C$_{Ar}$H), 139.85 (s, 1C, C$_{Ar}$Me), 160.1 (d, J_{PC} = 8.7, 2C, C$_{Ar}$OP), Anal. Calcd for $C_{19}H_{34}O_2P_2$ (356.42): C, 64.03; H, 9.62. Found: C, 63.83; H, 10.06.

1,3-(*i*-Pr$_2$PO)$_2$-5-COOMe-C$_6$H$_3$, 4. This ligand (a yellow oil) was prepared in 89% yield (4.23 g) using the same procedure described for the synthesis of **3**. ^{1}H NMR (400 MHz, $CDCl_3$): δ 1.09 (dd, J_{HP} = 16, J_{HH} = 7.2, 12H, CH(CH_3)$_2$), 1.16 (dd, J_{HP} = 10.8, J_{HH} = 7.0, 12H, CH(CH_3)$_2$), 1.91 (dh, J_{HP} = 2.4, J_{HH} = 7.1, 4H, PC*H*(CH$_3$)$_2$), 3.88 (s, 3H, OCH_3), 7.08 (m, J_{HP} = 2.0, 1H, *Ar*), 7.38 (m, 2H, *Ar*). ^{31}P{^{1}H} NMR (162 MHz, $CDCl_3$): δ 151.9 (s). ^{13}C{^{1}H} NMR (101 MHz, $CDCl_3$): δ 17. 0 (d, J_{CP} = 8.4, 4C, CH_3), 17.7 (d, J_{CP} = 20.1, 4C, CH_3), 28.3 (d, J_{CP}= 17.8, 4C, PCH(CH3)$_2$), 52.1 (s, 1C, OCH$_3$), 113.0 (d, J_{PC} = 10.8, 2C, 4,6-C$_{Ar}$), 113.4 (t, J_{PC} = 11.0, 1C, 2-C$_{Ar}$), 131.7 (s, 1C, C$_{Ar}$CO), 160.2 (d, J_{PC} = 9.1, 2C, C$_{Ar}$OP), 166.5 (s, 1C, C═O) Anal. Calcd for $C_{20}H_{34}O_4P_2$ (400.43): C, 59.99; H, 8.56. Found: C, 59.45; H, 8.66.

1,3-(*i*-Pr$_2$PO)$_2$-4-OMe-C$_6$H$_3$, 5. The standard procedure described for the synthesis of **3** gave a yellow oil after vacuum distillation (1.5 g, 60%). ^{1}H NMR (400 MHz, $CDCl_3$): δ 1.07 (dd, J_{HP} = 6.8, J_{HH} = 7.0, 6H, CH(CH_3)$_2$), 1.11 (dd, J_{HP} = 7.2, J_{HH} = 7.0, 6H, CH(CH_3)$_2$), 1.16 (dd, J_{HP} = 11.2, J_{HH} = 7.1, 6H, CH(CH_3)$_2$), 1.21 (dd, J_{HP} = 10.8, J_{HH} = 7.1, 6H, CH(CH_3)$_2$), 1.88 (dh, J_{HH} = 7.1, J_{HP} = 2.2, 2H, 3-OPC*H*(CH$_3$)$_2$), 1.94 (dh, J_{HH} = 7.1, J_{HP} = 1.8, 2H, 1-OPC*H*(CH$_3$)$_2$), 3.77 (s,OCH_3, 3H), 6.64 (dm(AB), J_{HH} = 9.4, 1H, 6-H$_{Ar}$), 6.72 (d(AB), J_{HH} = 8.8, 1H, 5-H$_{Ar}$), 6.98 (m, 1H, 2-H$_{Ar}$). ^{31}P{^{1}H} NMR (162 MHz, $CDCl_3$): δ 151.7 (s), 157.2 (s). ^{13}C{^{1}H} NMR (101 MHz, $CDCl_3$): δ 17.08 (d, J_{CP} = 8.6, 2C, CH_3), 17.17 (d, J_{CP} = 9.0, 2C, CH_3), 17.73 (d, J_{CP} = 8.4, 2C, CH_3), 17.93 (d, J_{CP} = 8.4, 2C, CH_3), 28.3 (d, J_{CP} = 17.9, 2C, PCH(CH$_3$)$_2$), 28.5 (d, J_{CP} = 18.5, 2C, PCH(CH$_3$)$_2$), 56.7 (s, 1C, OCH$_3$), 111.1 (dd, $J_{CP'}$ = 9.1, $J_{CP''}$ = 8.8, 1C, 2-C$_{Ar}$), 111.2 (d, J_{PC} = 10.7, 1C, 6-C$_{Ar}$), 113.3 (s, 1C, 5-C$_{Ar}$), 145.6 (s, 1C, C$_{Ar}$OMe), 149.0 (d, J_{PC} = 8.25, 1C, 1-C$_{Ar}$OP or 3-C$_{Ar}$OP), 153.4 (d, J_{PC} = 9.1, 1C, 3-C$_{Ar}$OP or 1-C$_{Ar}$OP). Anal. Calcd for $C_{19}H_{34}O_2P_2$ (372.42): C, 61.28; H, 9.20. Found: C, 60.97; H, 9.72.

1,3-(*i*-Pr$_2$PO)$_2$,4-(COOMe)-C$_6$H$_3$, 6. This ligand (a yellow oil) was prepared in 94% yield (4.5 g) using the same procedure described for the synthesis of **3**. ^{1}H NMR (400 MHz, $CDCl_3$): δ 1.03 (dd, J_{HP} = 16, J_{HH} = 7.2, 6H, CH(CH_3)$_2$), 1.10 (dd, J_{HP} = 15.6, J_{HH} = 7.2, 6H, CH(CH_3)$_2$), 1.17 (dd, J_{HP} = 10.8, J_{HH} = 7.0, 6H, CH(CH_3)$_2$), 1.31 (dd, J_{HP} = 10.8, J_{HH} = 7.0, 6H, CH(CH_3)$_2$), 1.81 (dh, J_{HH} = 7.1, J_{HP} = 2.8, 2H, 1-OPC*H*(CH$_3$)$_2$), 1.96 (dh, J_{HH} = 7.0, J_{HP}= 3.5, 2H, 3-OPC*H*(CH$_3$)$_2$), 3.65 (s, 3H, OCH_3), 6.92 (dm, J_{HH} = 8.7, 1H, 6-H$_{Ar}$), 7.87 (m, 1H, 2-H$_{Ar}$), 8.05 (d, J_{HH} = 8.7, 1H, 5-H$_{Ar}$). ^{31}P{^{1}H} NMR (162 MHz, $CDCl_3$): δ 151.1 (s), 151.6 (s). ^{13}C{^{1}H} NMR (75 MHz, $CDCl_3$): δ 16.88 (d, J_{CP} = 8.5, 2C, CH_3), 16.92 (d, J_{CP} = 8.5, 2C, CH_3), 17.41 (d, J_{CP} = 9.3, 2C, CH_3), 17.7 (d, J_{CP} = 10.1, 2C, CH_3), 28.14 (d, J_{CP} = 17.8, 2C, PCH(CH$_3$)$_2$), 28.2 (d, J_{CP} = 18.1, 2C, PCH(CH$_3$)$_2$), 51.36 (s, 1C, OCH$_3$), 108.3 (dd, $J_{CP'}$ = 12.7, $J_{CP''}$ = 11.8, 1C, 2-C$_{Ar}$), 110.9 (d, J_{PC} = 10.9, 1C, 6-C$_{Ar}$), 114.4 (s, *1C*, 5-C$_{Ar}$), 132.9 (s, 1C, C$_{Ar}$COOMe), 160.7 (d, J_{PC} = 9.2, 1C, 1-C$_{Ar}$OP or 3-C$_{Ar}$OP), 163.5 (d, J_{PC} = 8.5, 1C, 3-C$_{Ar}$OP or 1-C$_{Ar}$OP), 166.2 (s, 1C, C═O). Anal. Calcd for $C_{20}H_{34}O_4P_2$ (400,43): C, 59.99; H, 8.56. Found: C, 60.06; H, 8.61.

1,3-(*t*-Bu$_2$PO)-5-COOMe-C$_6$H$_3$, 9. This ligand was obtained as a colorless oil in 63% yield (1.7 g) using the same method as reported for ligand **8**.[15c] ^{1}H NMR (400 MHz, C_6D_6): δ 1.17 (d, J_{HP} = 11.7, C(CH_3)$_3$, 36H), 3.56 (s,OCH_3, 3H), 7.72 (m, *Ar*, 1H), 7.97 (m, *Ar*, 2H). ^{31}P{^{1}H} NMR (162 MHz, C_6D_6): δ 155.8 (s). ^{13}C{^{1}H} NMR (101 MHz, $CDCl_3$): δ 27.5 (d, J_{CP} = 15.6, 12C, CH_3), 35.8 (d, J_{CP} = 26.7, 4C, CCH_3), 51.8 (s, 1C, OMe), 113.1 (t, J_{PC} = 11.9, 1C, 2-C$_{Ar}$),

dx.doi.org/10.1021/om3009475 | *Organometallics* 2012, 31, 8561−8570

113.2 (d, J_{PC} = 10.8, 2C, 4,6-C_{Ar}), 133.0 (s, 1C, C_{Ar}CO), 161.4 (d, J_{PC} = 10.1, 2C, C_{Ar}OP), 166.3 (s, 1C, C═O) Anal. Calcd for $C_{24}H_{42}O_4P_2$ (456.54): C, 63.14; H, 9.27. Found: C, 63.75; H, 9.87.

Synthesis of the Complexes. Previously published reports have described the synthesis and characterization of complex **1′**[15Sb] and the chloro analogue of complex **8′**.[20] Slightly modified versions of these procedures were used to prepare all other complexes, as described below.

{2,6-(*i*-Pr$_2$PO)$_2$-4-OMe-C$_6$H$_2$}NiBr, 3′. To the solution of ligand **3** (1.05 g, 2.81 mmol) and NEt_3 (469 μL, 3.37 mmol) in THF (30 mL) was added $\{(i\text{-PrCN})NiBr_2\}_n$ (807 mg, 2.81 mmol), and the mixture was stirred at room temperature for one hour, during which it turned brown initially and then yellow, and a white precipitate appeared. Filtration of the final mixture and evaporation of the filtrate followed by extraction of the residual solids with hexane (3 × 25 mL) gave a solution that yielded yellow crystals by slow evaporation. Washing the crystals with a small quantity of cold hexane gave the desired product (0.81 g, 74%). ^{1}H NMR (400 MHz, C_6D_6): δ 1.18 (dt^v, J_{HH} = 4.3, 12H, CH(CH_3)$_2$), 1.40 (dt^v, J_{HH} = 6.1, 12H, CH(CH_3)$_2$), 2.26 (m, 4H, PC*H*(CH_3)$_2$), 3.25 (s, 3H,OCH_3), 6.33 (s, 2H, *Ar*). ^{31}P{^{1}H} NMR (162 MHz, C_6D_6): δ 190.63 (s). ^{13}C{^{1}H} NMR (101 MHz, $CDCl_3$): δ 16.79 (s, 4C, CH_3), 17.89 (s, 4C, CH_3), 28.29 (vt, J_{CP} = 11.2, 4C, P$CH(CH_3)_2$), 55.5 (s, 1C, OCH_3), 92.9 (vt, J_{PC} = 6.1, 2C, CH_{Ar}), 118.7 (t, J_{PC} = 21.4, 1C, Ni-C_{Ar}), 162.65 (s, 1C, C_{Ar}OMe), 169.5 (vt, J_{PC} = 10.4, 2C, C_{Ar}OP). UV−vis (CH_2Cl_2, 1.19 × 10^{-4} M) [λ_{max}, nm (ε, L mol^{-1} cm^{-1})]: 389(1748), 338(9895), 320(4876). Anal. Calcd for $C_{19}H_{33}O_3P_2NiBr$ (510.01): C, 44.75; H, 6.52. Found: C, 44.82; H, 6.46.

{2,6-(*i*-Pr$_2$PO)$_2$-4-Me-C$_6$H$_2$}NiBr, 2′. The standard procedure described above for **3′** gave the desired product as a yellow solid (1.05 g, 76%). ^{1}H NMR (300 MHz, $CDCl_3$): δ 1.33 (dt^v, J_{HH} = 7.0, J_{HP} = 6.7, CH(CH_3)$_2$, 12H), 1.43 (dt^v, J_{HH} = 8.3, J_{HP} = 8.0, (CH(CH_3)$_2$)$_2$, 12H), 2.20 (s,*CH*$_3$, 3H), 2.45 (m, J_{HH} = 6.8, 4H, PC*H*(CH_3)$_2$), 6.28 (s, *Ar*, 2H). ^{31}P{^{1}H} NMR (162 MHz, $CDCl_3$): δ 189.11 (s). ^{13}C{^{1}H} NMR (101 MHz, $CDCl_3$): δ 16.82 (s, 4C, CH_3), 17.88 (s, 4C, CH_3), 21.6 (s, 1C, CH_3), 28.07 (vt, J_{CP} = 11.3, 4C, P$CH(CH_3)_2$), 106.1 (vt, J_{PC} = 6.0, 2C, 3,5-C_{Ar}), 123.7 (t, J_{PC} = 21.5, 1C, Ni-C_{Ar}), 139.65 (s, 1C, C_{Ar}Me) 168.6 (vt, J_{PC} = 10.0, 2C, C_{Ar}OP). UV−vis (CH_2Cl_2, 13.56 × 10^{-4} M) [λ_{max}, nm (ε, L mol^{-1} cm^{-1})]: 396(164), 355(237), 338(1063), 324(517). Anal. Calcd for $C_{19}H_{33}O_2P_2NiBr$ (494.01): C, 46.19; H, 6.73. Found: C, 46.17; H, 6.66.

{2,6-(*i*-Pr$_2$PO)$_2$,4-(COOMe)C$_6$H$_2$}NiBr, 4′. The standard procedure described above for **3′** gave the desired product as a yellow solid (0.87 g, 92%). ^{1}H NMR (400 MHz, $CDCl_3$): δ 1.20 (dt^v, J_{HH} = 7.26 J_{HP} = 7.1, 12H, CH(CH_3)$_2$), 1.43 (dt^v, J_{HH} = 8.64 J_{HP} = 8.02, 12H, CH(CH_3)$_2$), 2.30 (m, 4H, PC*H*(CH_3)$_2$), 3.54 (s, 3H,OCH_3), 7.66 (s, 2H, *Ar*). ^{31}P{^{1}H} NMR (162 MHz, C_6D_6): δ 190.56 (s). ^{13}C{^{1}H} NMR (101 MHz, C_6D_6): δ 16.68 (s, 4C, CH_3), 17.75 (s, 4C, CH_3), 28.34 (vt, J_{CP} = 11.24, 4C, P$CH(CH_3)_2$), 51.7 (s, 1C, OCH_3), 106.8 (vt, 2C, CH_{Ar}), 131.9 (s, 1C, C_{Ar}COOMe), 137.19 (t, J_{PC} = 20.8, 1C, Ni-C_{Ar}), 166.6 (s, 1C, C═O), 169.0 (vt, J_{PC} = 10.0, 2C, C_{Ar}OP). UV−vis (CH_2Cl_2, 2.68 × 10^{-4} M) [λ_{max}, nm (ε, L mol^{-1} cm^{-1})]: 384(3863), 362(8552), 326(3118). Anal. Calcd for $C_{20}H_{33}O_4P_2NiBr$ (538.02): C, 44.65; H, 6.18. Found: C, 44.66; H, 6.49.

{2,6-(*i*-Pr$_2$PO)$_2$-3-OMe-C$_6$H$_2$}NiBr, 5′. The standard procedure described above for **3′** gave the desired product as a yellow solid (0.86 g, 90%). ^{1}H NMR (400 MHz, $CDCl_3$): δ 1.33−1.45 (m, 24H, CH(CH_3)$_2$), 2.45 (m, 2H, 3-OPC*H*(CH_3)$_2$), 2.51 (m, 2H, 1-OPC*H*(CH_3)$_2$), 3.77 (s, 3H, OCH_3), 6.35 (d (AB) J_{HH} = 7.25, 1H, 4-H_{Ar}), 6.61 (d (AB), J_{HH} = 7.18, 1H, 5-H_{Ar}). ^{31}P{^{1}H} NMR (162 MHz, $CDCl_3$): δ 187.5 (d, (AB) J_{PP} = 317.8, 1P), 192.2 (d, (AB) J_{PP} = 317.8, 1P). ^{13}C{^{1}H} NMR (101 MHz, $CDCl_3$): δ 16.79 (s, 2C, CH_3), 16.93 (s, 2C, CH_3), 17.86 (s, 2C, CH_3), 17.90 (s, 2C, CH_3), 28.16 (vt, J_{CP} = 19.1, 2C, P$CH(CH_3)_2$), 28.19 (vt, J_{CP} = 18.9, 2C, P$CH(CH_3)_2$), 57.2 (s, 1C, OCH_3), 103.9 (d, J_{PC} = 12.6, 1C, 5-C_{Ar}), 113.2 (s, 1C, 4-C_{Ar}), 129.7 (vt, J_{PC} = 20.4, 1C, Ni-C_{Ar}), 140.6 (d, J_{PC} = 13.9, 1C, MeOC_{Ar}), 156.9 (m, 1C, 2-C_{Ar}OP), 162.6 (dd, 1C, 6-C_{Ar}OP). UV−vis (CH_2Cl_2, 6.47 × 10^{-4} M) [λ_{max}, nm (ε, L mol^{-1} cm^{-1})]: 394(153), 358(170), 339(852). Anal. Calcd for $C_{19}H_{33}O_3P_2NiBr$ (510.01): C, 44.75; H, 6.52. Found: C, 45.11; H, 6.59.

{2,6-(*i*-Pr$_2$PO)$_2$-3-COOMe-C$_6$H$_2$}NiBr, 6′. The standard procedure described above for **3′** gave the desired product as a yellow solid (0.81 g, 86%). ^{1}H NMR (300 MHz, C_6D_6): δ 1.11 (dt^v, J_{HH} = 7.63, 7.03, 6H, CH(CH_3)$_2$), 1.21 (dt^v, J_{HH} = 7.8, J_{HP} = 6.8, 6H, CH(CH_3)$_2$), 1.33 (dt^v, J_{HH} = 7.4, J_{HP} = 7.4, 6H, CH(CH_3)$_2$), 1.36 (dt^v, J_{HH} = 7.5, J_{HP} = 7.5, 6H, CH(CH_3)$_2$), 2.20 (dh, J_{HH} = 5.3, J_{HP} = 1.6, 2H, 6-OPC*H*(CH_3)$_2$), 2.29 (dh, J_{HH} = 5.1, J_{HP} = 1.7, 2H, 2-OPC*H*(CH_3)$_2$), 3.53 (s, 3H, OCH_3), 6.52 (d J_{HH} = 8.5, 1H, 5-H_{Ar}), 7.88 (d, J_{HH} = 8.4, 1H, 4-$C_{Ar}H$). ^{31}P{^{1}H} NMR (202 MHz, C_6D_6): δ 190.4 (d, (AB) J_{PP} = 323, 1P), 192.1 (d, (AB) J_{PP} = 323, 1P). ^{13}C{^{1}H} NMR (75 MHz, C_6D_6): δ 16.66 (s, 2C, CH_3), 16.81 (s, 2C, CH_3), 17.73 (t, J_{CP} = 2.4, 2C, CH_3), 17.83 (t, J_{CP} = 2.4, 2C, CH_3), 28.27 (vt, J_{CP} = 12.4, 2C, PCH(CH3)$_2$), 28.41 (vt, J_{CP}= 13.4, 2C, PCH(CH3)$_2$), 51.27 (s, 1C, OCH_3), 106.1 (dd, $J_{P'C}$ = 5.3, $J_{P''C}$ = 5.1, 1C, 5-C_{Ar}), 110.62 (dd, $J_{P'C}$ = 5.3, $J_{P''C}$ = 5.5, 1C, C_{Ar}C═O), 131.33 (vt, J_{PC} = 20.1, 1C, Ni-C_{Ar}), 132.77 (s, 1C, 4-C_{Ar}), 165.37 (s, 1C, C═O), 168.71 (t, J_{CP} = 10.5, 1C, 6-C_{Ar}OP), 172.0 (t, J_{CP} = 10.2, 1C, 2-C_{Ar}OP). UV−vis (CH_2Cl_2, 6.88 × 10^{-4} M) [λ_{max}, nm (ε, L mol^{-1} cm^{-1})]: 397(157), 360(201), 343(776). Anal. Calcd for $C_{20}H_{33}O_4P_2NiBr$ (538.02): C, 44.65; H, 6.18. Found: C, 44.56; H, 6.15.

{2,6-(*i*-Pr$_2$PO)$_2$-3,5-*t*-Bu$_2$-C$_6$H}NiBr, 7′. The standard procedure described above for **3′** gave the desired product as a yellow solid (577 mg, 45%). ^{1}H NMR (400 MHz, C_6D_6): δ 1.33 (s, 18H, C(CH_3)$_3$), 1.36 (dt^v, J_{H-H} = 10.8, $^vJ_{H-P}$ = 7.3, 12H, CH_3), 1.44 (dt^v, J_{H-H} = 8.3, $^vJ_{H-P}$ = 7.6, 12H, CH_3), 2.48 (m, 4H, PC*H*(CH_3)$_2$), 6.92 (s, 1H, H_{Ar}). ^{31}P{^{1}H} NMR (162 MHz, C_6D_6): δ 185.15 (s). ^{13}C{^{1}H} NMR (101 MHz, $CDCl_3$): δ 17.08 (s, 4C, CH_3), 18.01 (t^v, J_{CP} = 2.48, 4C, CH_3), 28.18 (t^v, J_{CP} = 11.8, 4C, PCH(CH3)$_2$), 30.06 (s, 6C, C(CH_3)$_3$), 34.41 (s, 2C, $C(CH_3)_3$), 123.89 (s, 1C, CH_{Ar}), 126.52 (t^v, J_{CP} = 5.17, 2C, C_{Ar}(^{t}Bu)), 131.28 (t, J_{PC}=19.8, 1C, Ni-C_{Ar}), 164.15 (t^v, J_{PC} = 9.55, 2C, C_{Ar}OP). UV−vis (CH_2Cl_2, 3.68 × 10^{-4} M) [λ_{max}, nm (ε, L mol^{-1} cm^{-1})]: 389(1622), 355(1987), 338(8923), 325(5378), 307 (3445) Anal. Calcd for $C_{26}H_{47}O_2P_2NiBr$ (592.20): C, 52.73; H, 8.00. Found: C, 53.06; H, 8.08.

{2,6-(*t*-Bu$_2$PO)$_2$-C$_6$H$_3$}NiBr, 8′. The standard procedure described above for **3′** gave the desired product as a yellow solid (0.4 g, 57%). ^{1}H NMR (400 MHz, C_6D_6): δ 1.46 (vt, J_{HP} = 6.6, 36H, CH_3), 6.6 (d, J_{HH} = 7.8, 2H, H_{Ar}), 6.88 (t, J_{HH} = 7.6, 1H, H_{Ar}). ^{31}P{^{1}H} NMR (162 MHz, C_6D_6): δ 191.00 (s). ^{13}C{^{1}H} NMR (101 MHz, $CDCl_3$): δ 27.39 (s, 12C, CH_3), 38.75 (vt, J_{CP} = 7.1, 4C, PC), 103.84 (vt, J_{CP} = 5.6, 2C, 3,5-C_{Ar}), 126.14 (t, J_{CP} = 20.0, 1C, Ni-C_{Ar}), 127.37 (s, 1C, 4-C_{Ar}) 168.38 (vt, J_{PC} = 9.4, 1C, C_{Ar}OP). UV−vis (CH_2Cl_2, 4.51 × 10^{-4} M) [λ_{max}, nm (ε, L mol^{-1} cm^{-1})]: 407(198), 352(138), 334(916). Anal. Calcd for $C_{20}H_{33}O_4P_2NiBr$ (536.09): C, 49.29; H, 7.33. Found: C, 49.28; H, 7.39.

{2,6-(*t*-Bu$_2$PO)$_2$-4-COOMe-C$_6$H$_2$}NiBr, 9′. The standard procedure described above for **3′** gave the desired product as a yellow solid (0.94 g, 72%). ^{1}H NMR (400 MHz, C_6D_6): δ 1.41 (vt, J_{HP} = 6.1, CH_3, 36H), 3.50 (s, 3H, OCH_3), 7.45 (s, 2H, H_{Ar}). ^{31}P{^{1}H} NMR (162 MHz, C_6D_6): δ 191.81 (s). ^{13}C{^{1}H} NMR (101 MHz, $CDCl_3$): δ 28.27 (s, 12C, CH_3), 39.94 (vt, J_{CP} = 6.9, 4C, PC(CH3)$_3$), 52.06 (s, 1C, OCH_3), 105.86 (vt, J_{CP} = 5.3, 2C, 3,5-C_{Ar}), 130.48 (s, 1C, C_{Ar}COOMe), 135.91 (t, J_{PC} = 19.0, 1C, Ni-C_{Ar}), 167.04 (s, 1C, C═O), 169.0 (vt, J_{PC} = 8.9, 2C, C_{Ar}OP). UV−vis (CH_2Cl_2, 10.6 × 10^{-4} M) [λ_{max}, nm (ε, L mol^{-1} cm^{-1})]: 413(228), 360(1043), 326(378). Anal. Calcd for $C_{20}H_{33}O_4P_2NiBr$ (594.12): C, 48.52; H, 6.96. Found: C, 48.64; H, 7.16.

Cyclic Voltammetry Experiments. Cyclic voltammetry measurements were performed using a SP50 BioLogic Science Instrument potentiostat. A typical three-electrode system consisting of a graphite working electrode, a Pt auxiliary electrode, and a Ag/AgCl reference electrode was employed. The experiments were carried out at room temperature on analyte solutions prepared in dry CH_2Cl_2 containing [*n*-Bu_4N][PF_6] as electrolyte (0.1 M). The samples were bubbled with nitrogen before each experiment. Under the experimental conditions of our studies, the redox potential ($E_{1/2}$) for the Cp_2Fe^+/Cp_2Fe couple was +0.43 V.

Crystal Structure Determinations. The crystallographic data for compounds **2′**, **4′**, and **8′** were collected on a Bruker Microstar

generator (Microsource) equipped with a Helios optics, a Kappa Nonius goniometer, and a Platinum135 detector. The crystallographic data for complexes **3′**, **8**, and **9′** were collected on a Nonius FR591 generator (rotating anode) equipped with a Montel 200, a D8 goniometer, and a Bruker Smart 6000 area detector. The crystallographic data for complexes **7′** were collected on a a Bruker APEX II equipped with an Incoatec I\muS Microsource and a Quazar MX monochromator. Cell refinement and data reduction were done using SAINT.[28] An empirical absorption correction, based on the multiple measurements of equivalent reflections, was applied using the program SADABS.[29] The space group was confirmed by XPREP routine[30] in the program SHELXTL.[31] The structures were solved by direct methods and refined by full-matrix least-squares and difference Fourier techniques with SHELX-97.[32] All non-hydrogen atoms were refined with anisotropic displacement parameters. Hydrogen atoms were set in calculated positions and refined as riding atoms with a common thermal parameter.

■ ASSOCIATED CONTENT

Supporting Information

Tables of NMR data (^{1}H and ^{13}C{^{1}H}) for ligands and complexes, a plot correlating ^{31}P chemical shifts for ligands and complexes, tables of crystal data and collection/refinement parameters, and a table of absorption spectral data for ligands and complexes. This material is available free of charge via the Internet at http://pubs.acs.org. Complete details of the X-ray analyses reported herein have been deposited at The Cambridge Crystallographic Data Centre (CCDC 895773 (**8**), 895779 (**2′**), 895774 (**3′**), 895778 (**4′**), 895776 (**7′**), 895777 (**8′**), 895775 (**9′**)). This data can be obtained free of charge via www.ccdc.cam.ac.uk/data_request/cif, or by e-mailing data_request@ccdc.cam.ac.uk, or by contacting The Cambridge Crystallographic Data Centre, 12 Union Road, Cambridge CB2 1EZ, UK; fax: +44 1223 336033.

■ AUTHOR INFORMATION

Corresponding Author

*E-mail: zargarian.davit@umontreal.ca.

Notes

The authors declare no competing financial interest.

■ ACKNOWLEDGMENTS

The authors are grateful to NSERC of Canada for a Discovery Grant to D.Z., Université de Montréal and Centre in Green Chemistry and Catalysis for graduate fellowships to B.V., Dr. Laure Benhamou for valuable discussions, Mr. Olivier Marcadet for technical assistance with some of the experiments, and Dr. Michel Simard and Ms. Francine Bélanger-Gariépy for their valuable assistance with crystallography.

■ REFERENCES

(1) Moulton, C. J.; Shaw, B. L. *J. Chem. Soc., Dalton Trans.* **1976**, 1020.

(2) (a) Grove, D. M.; van Koten, G.; Zoet, R. *J. Am. Chem. Soc.* **1983**, *105*, 1379. (b) Grove, D. M.; van Koten, G.; Ubbels, H. J. C.; Zoet, R. *Organometallics* **1984**, *3*, 1003.

(3) (a) van Koten, G. *Pure Appl. Chem.* **1989**, *61*, 1681. (b) Albrecht, M.; van Koten, G. *Angew. Chem., Int. Ed.* **2001**, *40*, 3750. (c) Gossage, R. A.; van de Kuil, L. A.; van Koten, G. *Acc. Chem. Res.* **1998**, *31*, 423. (d) Zargarian, D.; Castonguay, A.; Spasyuk, D. M. ECE-Type Pincer Complexes of Nickel. *Top. Organomet. Chem.* **2013**, *40*, 131−173.

(4) (a) Castonguay, A.; Sui-Seng, C.; Zargarian, D.; Beauchamp, A. L. *Organometallics* **2006**, *25*, 602. (b) Castonguay, A.; Beauchamp, A. L.; Zargarian, D. *Organometallics* **2008**, *27*, 5723.

(5) (a) Gómez-Benítez, V.; Baldovino-Pantaleón, O.; Herrera-Álvarez, C.; Toscano, R. A.; Morales-Morales, D. *Tetrahedron Lett.* **2006**, *47*, 5059. (b) Pandarus, V.; Zargarian, D. *Chem. Commun.* **2007**, 978. (c) Pandarus, V.; Zargarian, D. *Organometallics* **2007**, *26*, 4321. (d) Salah, A. B.; Zargarian, D. *Dalton Trans.* **2011**, *40*, 8977. (e) Salah, A. B.; Offenstein, C.; Zargarian, D. *Organometallics* **2011**, *30*, 5352. (f) Lefèvre, X.; Durieux, G.; Lesturgez, S.; Zargarian, D. *J. Mol. Catal. A: Chem.* **2011**, *335*, 1. (g) Xu, G.; Li, X.; Sun, H. *J. Organomet. Chem.* **2011**, *696*, 3011.

(6) (a) Spasyuk, D. M.; van der Est, A.; Zargarian, D. *Organometallics* **2009**, *28*, 6531. (b) Spasyuk, D. M.; Zargarian, D. *Inorg. Chem.* **2010**, *49*, 6203. (c) Zhang, B.-S.; Wang, W.; Shao, D.-D.; Hao, X.-Q.; Gong, J.-F.; Song, M.-P. *Organometallics* **2010**, *29*, 2579. (d) Niu, J.-L.; Chen, Q.-T.; Hao, X.-Q.; Zhao, Q.-X.; Gong, J.-F.; Song, M.-P. *Organometallics* **2010**, *29*, 2148. (e) Spasyuk, D. M.; Gorelsky, S. I.; van der Est, A.; Zargarian, D. *Inorg. Chem.* **2011**, *50*, 2661. (f) Yang, M.-J.; Liu, Y.-J.; Gong, J.-F.; Song, M.-P. *Organometallics* **2011**, *30*, 3793. (g) Sanford, J.; Dent, C.; Masuda, J. D.; Xia, A. *Polyhedron* **2011**, *30*, 1091.

(7) (a) Fan, L.; Foxman, B. M.; Ozerov, O. V. *Organometallics* **2004**, *23*, 326. (b) Ozerov, O. V.; Guo, C.; Fan, L.; Foxman, B. M. *Organometallics* **2004**, *23*, 5573. (c) Liang, L.-C.; Chien, P.-S.; Huang, Y.-L. *J. Am. Chem. Soc.* **2006**, *128*, 15562. (d) Liang, L.-C.; Chien, P.-S.; Lin, J.-M.; Huang, M.-H.; Huang, Y.-L.; Liao, J.-H. *Organometallics* **2006**, *25*, 1399. (e) Adhikari, D.; Huffman, J. C.; Mindiola, D. J. *Chem. Commun.* **2007**, 4089. (f) Adhikari, D.; Mossin, S.; Basuli, F.; Huffman, J. C.; Szilagyi, R. K.; Meyer, K.; Mindiola, D. J. *J. Am. Chem. Soc.* **2008**, *130*, 3676. (g) Adhikari, D.; Pink, M.; Mindiola, D. J. *Organometallics* **2009**, *28*, 2072.

(8) (a) Vechorkin, O.; Proust, V.; Hu, X. *J. Am. Chem. Soc.* **2009**, *131*, 9756. (b) Madhira, V. N.; Ren, P.; Vechorkin, O.; Hu, X.; Vicic, D. A. *Dalton Trans.* **2012**, *41*, 7195. (c) Breitenfeld, J.; Scopelliti, R.; Hu, X. *Organometallics* **2012**, *31*, 2128.

(9) (a) Chakraborty, S.; Krause, J. A.; Guan, H. *Organometallics* **2009**, *28*, 582. (b) Chakraborty, S.; Patel, Y. J.; Krause, J. A.; Guan, H. *Polyhedron* **2012**, *32*, 30. (c) Zhang, J.; Medley, C. M.; Krause, J. A.; Guan, H. *Organometallics* **2010**, *29*, 6393. (d) Chakraborty, S.; Zhang, J.; Krause, J. A.; Guan, H. *J. Am. Chem. Soc.* **2010**, *132*, 8873. (e) Huang, F.; Zhang, C.; Jiang, J.; Wang, Z.-X.; Guan, H. *Inorg. Chem.* **2011**, *50*, 3816.

(10) (a) Boro, B. J.; Duesler, E. N.; Goldberg, K. I.; Kemp, R. A. *Inor. Chem.* **2009**, *48*, 5081. (b) Schmeier, T. J.; Hazari, N.; Incarvitoa, C. D.; Raskatovb, J. A. *Chem. Commun.* **2011**, *47*, 1824. (c) Rossin, A.; Peruzzini, M.; Zanobini, F. *Dalton Trans.* **2011**, *40*, 4447.

(11) (a) Castonguay, A.; Spasyuk, D. M.; Madern, N.; Beauchamp, A. L.; Zargarian, D. *Organometallics* **2009**, *28*, 2134. (b) Castonguay, A.; Beauchamp, A. L.; Zargarian, D. *Inorg. Chem.* **2009**, *48*, 3177.

(12) Solano-Prado, M. A.; Estudiante-Negrete, F.; Morales-Morales, D. *Polyhedron* **2010**, *29*, 592.

(13) Estudiante-Negrete, F.; Hernàndez-Ortega, S.; Morales-Morales, D. *Inorg. Chim. Acta* **2012**, *387*, 58.

(14) Chen, T.; Yang, L.; Li, L.; Huang, K.-W. *Tetrahedron* **2012**, *68*, 6152.

(15) (a) Zhu, K.; Achord, P. D.; Zhang, X.; Krogh-Jespersen, K.; Goldman, A. S. *J. Am. Chem. Soc.* **2004**, *126*, 13044. (b) Göttker-Schnetmann, I.; White, P. S.; Brookhart, M. *Organometallics* **2004**, *23*, 1766. (c) Göttker-Schnetmann, I.; White, P.; Brookhart, M. *J. Am. Chem. Soc.* **2004**, *126*, 1804. (d) Huang, Z.; Brookhart, M.; Goldman, A. S.; Kundu, S.; Ray, A.; Scott, S. L.; Vicente, B. C. *Adv. Synth. Catal.* **2009**, *351*, 188. (e) Polukeev, A. V.; Kuklin, S. A.; Petrovskii, P. V.; Peregudov, A. S.; Dolgushin, F. M.; Ezernitskaya, M. G.; Koridze, A. A. *Russ. Chem. Bull., Int. Ed.* **2010**, *59*, 745.

(16) (a) van de Kui1, L. A.; Luitjes, H.; Grove, D. M.; Zwikker, J. W.; van der Linden, J. G. M.; Roelofsen, A. M.; Jenneskens, L. W.; Drenth, W.; van Koten, G. *Organometallics* **1994**, *13*, 468−477. (b) Slagt, M. Q.; RodrÌguez, G.; Grutters, M. M. P.; Gebbink, R. J. M. K.; Klopper, W.; Jenneskens, L. W.; Lutz, M.; Spek, A. L.; van Koten, G. *Chem.—Eur. J.* **2004**, *10*, 1331−1344.

(17) For the original reports on preparation of POC^{H}OP-type ligands see: (a) Bedford, R. B.; Draper, S. M.; Scully, P. N.; Welch, S. L. *New J. Chem.* **2000**, *24*, 745. (b) Morales-Morales, D.; Grause, C.; Kasaoka, K.; Redon, R.; Cramer, R. E.; Jensen, C. M. *Inorg. Chim. Acta* **2000**, *300*−*302*, 958.
(18) A recent study has shown that nickellation of the central C-H moiety in these POCOP ligands proceeds by an electrophilic mechanism: Vabre, B.; Lambert, M. L.; Petit, A.; Ess, D. H.; Zargarian, D. *Organometallics* **2012**, *31*, 6041.
(19) In the case of low-yielding reactions, NMR spectra of the final reaction mixtures did not show any unreacted ligands. We have no definitive explanation at this point for the observed low yields other than the possibility that the chelated intermediates formed in these cases decompose into intractable dimeric or polymeric species instead of proceeding to nickellation. For a discussion of related reactions leading to non-metallated species see: Pandarus, V.; Castonguay, A.; Zargarian, D. *J. Chem. Soc., Dalton Trans.* **2008**, 4756−4761.
(20) Canet, D.; Boudel, J. C.; Canet Soula, E. *La RMN: Concepts, Méthodes et applications*, 2nd ed.; Dunod: Paris, 2002.
(21) Schwartsburd, L.; Poverenov, E.; Shimon, L. J. W.; Milstein, D. *Organometallics* **2007**, *26*, 2931.
(22) The synthesis and solid-state structure of the chloro analogue of complex **8′** have been reported previously: ref 9a.
(23) The following alternative interpretations have been suggested by reviewers of our manuscript to explain the shorter Ni−Br distances observed in complexes **4′** and **9′**: the electron-withdrawing substituent CO_2Me present in these complexes tends to create a more polarized Ni−C_{ispo} interaction in the direction of C_{ipso}, thus enhancing both the Coulombic interaction between Ni^+ and Br^- and/or the extent of Br→Ni π-donation.
(24) (a) Jude, H.; Bauer, J. A. K.; Connick, W. B. *Inorg. Chem.* **2002**, *41*, 2275. (b) Jude, H.; Bauer, J. A. K.; Connick, W. B. *Inorg. Chem.* **2004**, *43*, 725. (c) Jude, H.; Bauer, J. A. K.; Connick, W. B. *Inorg. Chem.* **2005**, *44*, 1211.
(25) The fairly significant impact of *para*-substituents on the observed redox rules out the possibility of the observed redox events occurring on the PR_2 moieties.
(26) Foti, M. C.; Daquino, C.; Mackie, I. D.; DiLabio, G. A.; Ingold, K. U. *J. Org. Chem.* **2008**, *73*, 9270.
(27) Bedford, R. B.; Betham, M.; Blake, M. E.; Coles, S. J.; Draper, S. M.; Hursthouse, M. B.; Scully, P. N. *Inorg. Chim. Acta* **2006**, *359*, 1870.
(28) *SAINT*, Release 6.06; Integration Software for Single Crystal Data; Bruker AXS Inc.: Madison, WI, 1999.
(29) Sheldrick, G. M. *SADABS*, Bruker Area Detector Absorption Corrections; Bruker AXS Inc.: Madison, WI, 1999.
(30) *XPREP*, Release 5.10; X-ray Data Preparation and Reciprocal Space Exploration Program; Bruker AXS Inc.: Madison, WI, 1997.
(31) *SHELXTL*, Release 5.10; The Complete Software Package for Single Crystal Structure Determination; Bruker AXS Inc.: Madison, WI, 1997.
(32) (a) Sheldrick, G. M. *SHELXS97*, Program for the Solution of Crystal Structures; Univ. of Gottingen: Germany, 1997. (b) Sheldrick, G. M. *SHELXL97*, Program for the Refinement of Crystal Structures; University of Gottingen: Germany, 1997.